Technical Annals

Vol 1, No 1 (2022)

Technical Annals

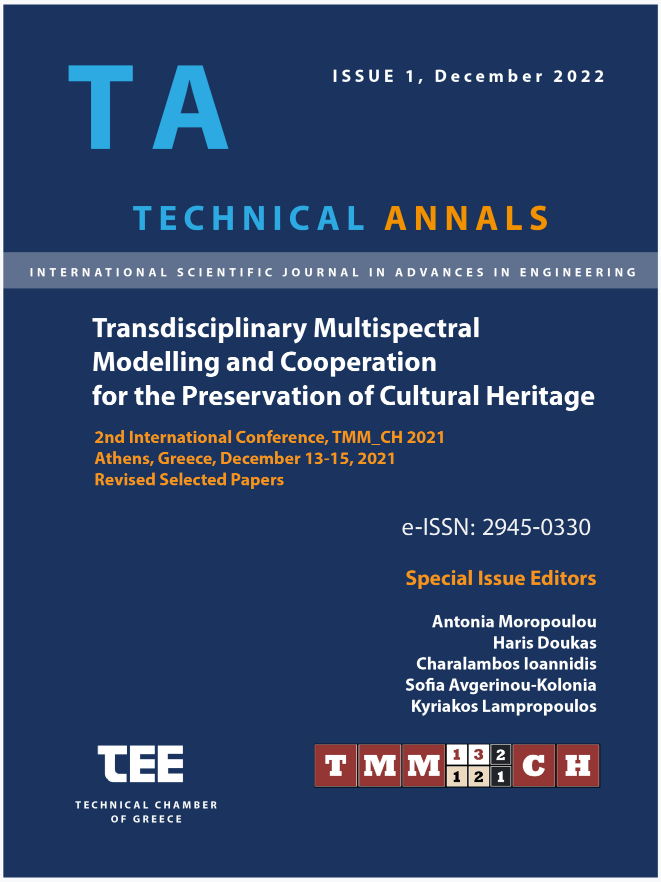

Non-destructive 3D reconstruction of an Hagia Sophia clone mosaic utilizing ultrasonography combined with an accurate motion planning

Stamatios Amanatiadis, Georgios Karagiannis, Evdoxios Mimis

doi: 10.12681/ta.32174

Non-destructive 3D reconstruction of an Hagia Sophia clone mosaic utilizing ultrasonography combined with an accurate motion planning [24]

Stamatios Amanatiadis[1[0000−0003−1295−4613]], Georgios Karagiannis[1,2[0000−0001−9847−6354]], and Evdoxios Mimis[1]

[1] Art Diagnosis Centre,"ORMYLIA" Foundation, Ormylia, GR-63071, Greece
[2]Diagnosis Multisystems, Nea Moudania, GR-63200, Greece
amanatiadis@artdiagnosis.gr,
g.karagiannis}@artdiagnosis.gr
engineering@diagnosismultisystems.eu

Abstract. In the current work the endoscopy and retrieval of mortar covered mosaic patterns, such as the Hagia Sophia ones, is presented. In particular, an appropriate instrumentation is developed combining ultrasonic tomography and an accurate motion planning. The acquisition of high-response tomographic images is performed utilizing transducers in a linear array through the efficient control of their phase characteristics both in transmit and receive modes. Moreover, an accurate mechanical adaptation is designed in order to move the ultrasonic probe with a constant velocity. Then, a sequence of tomographic images is recorded and the 3D endoscopic characteristics of the measured object are extracted via the effective reconstruction of the 3D volume. This device is used on a realistic Hagia Sophia mosaic replica that is covered by a thick mortar layer. The evaluated results indicate a complete 3D reconstruction of the hidden mosaic in micrometric resolution, while the inner details of individual tesserae are, also, recovered.

Keywords: beam forming mosaic tessera tomography.

1 Introduction

During the recent history of cultural heritage science, various techniques from physics, chemistry and engineering have been utilized for the identification of the material and structural composition of an artwork [3]. A notable example is the utilization

[24] Funded from the European Union Horizon 2020 Framework Programme.

of ultrasound tomography for surface mapping and stratigraphy extraction of an object that is under investigation [2]. Specifically, ultrasonic transducers in a linear array are able to support the high-response tomographic image reconstruction through the efficient manipulation of their phase-shift both in transmit and receive mode. However, single tomographic images are not adequate to reveal the complete structure of the examined object, thus a 3D approach is required. Such a case is the Hagia Sophia mosaics that are covered with a thick mortar layer and the reconstruction of their pattern, in a non-destructive manner, is required to unveil iconic Byzantine art aspects

In this paper, we present an integrated platform that combines ultrasonic tomography with accurate mechanical adaptations for the non-destructive 3D endoscopy of Hagia Sophia clone mortar-covered mosaics in order to retrieve their pattern. Initially, a functional, versatile and multi-degree of freedom linear array of ultrasonic transducers is examined in terms of the required phase-shift to achieve the high-response single tomographic imaging. Then, the appropriate mechanical adaptations are designed for the accurate motion of the ultrasonic probe via constant velocity. The sequence of the tomographic images is recorded throughout the entire motion of the probe, while the 3D image reconstruction is achieved considering the ratio of the constant velocity to the image resolution. The proposed instrumentation is, then, used on a realistic Hagia Sophia mosaic replica, covered by a thick mortar layer. The ultrasonic tomography acquisition and the subsequent 3D reconstruction reveals a high fidelity hidden mosaic pattern with an image resolution that is in a micrometric order.

2 Instrumentation

2.1 Phased array for tomographic image acquisition

Principle of operation The phased array probe consists of N small ultrasonic transducers, each of which can be pulsed independently. By varying the timing, for instance by making the pulse from each transducer progressively delayed going up the line, a pattern of constructive interference is set up that results in radiating a quasi-plane ultrasonic beam at a set angle depending on the progressive time delay. In other words, by changing the progressive time delay the beam can be steered electronically. It can be swept like a search-light through the tissue or object being examined, and the data from multiple beams are put together to make a visual image showing a slice through the object. Moreover, focusing of the transmitted beam can be accomplished by combining a parabolic timing relationship with a linear one to produce a beam which is focused at a given range and propagated at a specific angle. The following generalized focusing formula is derived to compute the required time delays

$$t_n = \frac{F}{c}\left[\sqrt{1+\left(\frac{\tilde{N}d}{F}\right)^2+\frac{2\tilde{N}d}{F}\sin\theta}-\sqrt{1+\left(\frac{(n-\tilde{N})d}{F}\right)^2-\frac{2(n-\tilde{N})d}{F}\sin\theta}\right] \quad (1)$$

where t_n is the required time delay for element $n = 0, \dots, N - 1$, $\tilde{N} = (N - 1)/2$, d is the center-to-center spacing between elements, F is the focal length from the center of the array, ϑ is the steering angle from the center of array and c the speed of sound. This generalized focusing time delay formula is valid for any number of array elements (even or odd), while by eliminating the constant t_0, the formula guarantees positive time delays which do not have to be larger than necessary

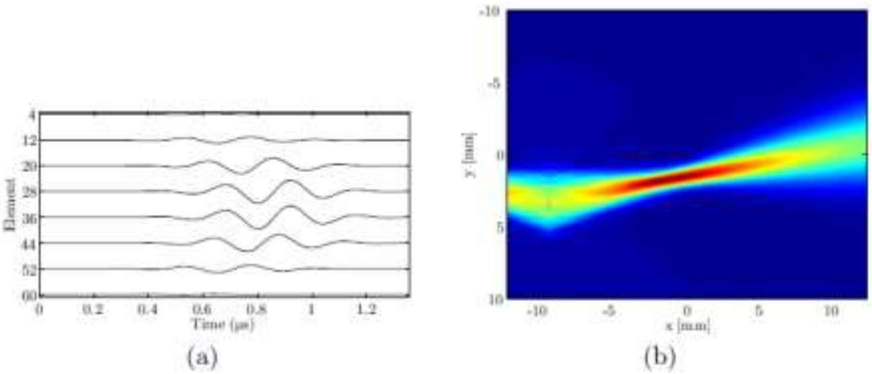

Fig. 1. (a) Stimulation signals and (b) amplitude of pressure of a linear phased array achieving a beam that is directed towards 10◦ and focused at 10 mm applying a Hann weighting function for apodization.

One major problem of phased array excitation is the "sidelobes" that can appear to be false echoes of the beam profile region. For this reason, apodization techniques are utilized by weighting the amplitude of the normal velocity across the array. Specifically, it is accomplished by simply exciting individual elements in the array with different voltage amplitudes, defined by popular weighting functions such as Hann

$$w_h[n] = \sin^2\left(\frac{\pi n}{N}\right), \qquad 0 \leqslant n \leqslant N, \tag{2}$$

or gaussian

$$w_g[n] = \mathrm{e}^{\frac{(n-\bar{N})^2}{2\alpha^2}}, \tag{3}$$

where α a properly defined constant. A simple scenario of a phased array transducer is numerically investigated [8], where 64 piezoelectric elements are utilized and stimulated so that the beam is directed towards 10◦ and focused at 10 mm from the phased array center, while a Hann weighting function is used for apodization. Some selected signals are sketched in Fig. 1 and the extracted pressure amplitude in Fig. 1 proves the successful implementation of the desired characteristics.

Multi-line acquisition beam forming An interesting observation is that the beam does not need to be the same in the transmit and receive phase and this is certainly the case with multiline acquisition beam forming. The basic idea behind this approach is to transmit a wide beam, so that a large area is insonificated, and then make use in receive of multiple, narrower beams, in order to form several A-scans along different directions for each transmission event. In this way, multiple lines are formed in parallel, thus increasing the frame rate and improving the temporal resolution. The receive phase is in fact defined by how the different signals received by all of the array elements are combined to form a line of the image

Therefore, it is possible to apply different phase sets and apodization masks to the signals received after a single transmission event, thus allowing the formation of multiple lines in parallel at varying focusing points. The combination through image fusion of the multiple images is able to enhance significantly the quality of the final tomographic image. It is evident that a wider beam can be achieved by using, without focusing, a small subaperture at the center of the array during transmission [5–7, 9].

The multiline acquisition method can be applied efficiently to achieve a gain in the frame rate, it can also be applied to improve the signal-to-noise ratio and contrast by simply averaging consecutive images obtained at a higher temporal resolution than with standard beam forming (i.e., techniques where only one line is generated per transmission event). Moreover, it can also be used to image a larger field of view. In this case, the gain in acquisition rate is used to widen the area covered by the imaging system. To summarize, image lines could be formed in parallel, meaning that

- the temporal resolution can be improved,
- consecutive images can be fused to enhance the quality,
- a larger field of view can be established,
- a combination of these gains could be achieved by spending the higher data acquisition rate in the most desirable way (e.g., fusion of less consecutive images and thus improving the signal-to-noise ratio while still improving also the frame rate).

2.2 Mechanical adaptations for volume acquisition

As it is described in the previous section, a linear phased array is capable of acquiring tomographic images at high data rate. It is evident that a possible combination of consecutive images at slightly different positions, as depicted in Fig. 2

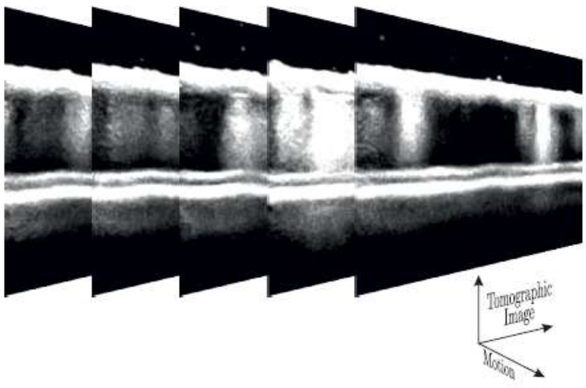

Fig. 2. Acquisition of consecutive tomographic images via the controlled motion of the linear phased array.

can provide a measurement of an entire 3D region of interest. This is achieved using a precise mechanical adaptation for the motion of the phased array parallel to the tomographic image normal vector with a constant velocity v [mm/sec]. Furthermore, considering a constant frame rate f_r [frames/sec] of tomographic image acquisition, the number of frames per distance is straight- forwardly calculated

$$\frac{\text{frames}}{\text{mm}} = \frac{f_r}{v}. \tag{4}$$

Now, this value must be connected to the resolution [pixel/mm] of any single tomographic image (that is defined straightforwardly via the ultrasonic measure- ment) by enforcing

$$\frac{\text{pixels}}{\text{mm}} \equiv \frac{\text{frames}}{\text{mm}}. \tag{5}$$

Obviously, these values may not be identical and consequently the initial tomographic images are resized by the factor

$$\alpha = \frac{f_r}{v\frac{\text{pixels}}{\text{mm}}}. \tag{6}$$

Finally, the images are combined into a single file that is fully compatible to the DICOM format, following the DICONDE standard [1] and extending its proper- ties by inserting modality-specific information, when necessary. The DICONDE standard was developed by the Non-Destructive Testing/Evaluation (NDT or NDE) community to reduce the cost of storage, making it easy to share and compare imaging information and enabling quantitative analysis. This way, the produced volumes can be loaded into third-party processing, medical and NDT software platforms with ease, such as 3D-SLICER [4], MITK [10] and MatlabTM for postprocessing and visualization purposes.

3 Operational Analysis

3.1 Test-case description

The operational status of the proposed instrumentation is examined and validated using a specific test case scenario including a mosaic pattern that is covered by thick mortar, as demonstrated in Fig.3. Initially, a preparation layer is placed and the mosaic, that simulates realistically the technique of the ones in Hagia Sophia, Constantinople, is designed over it. The utilized tesserae are, also, formed to approximate the real ones, in terms of their dimensions and structure. Finally, a 1 cm thick mortar is placed to cover entirely the designed mosaic.

3.2 Non-destructive acquisition of 3D sub-surface details

The structure of the clone mosaic is measured using the proposed methodology. A SuperSonic Imagine Aixplorer ultrasonic system is employed with a probe of central frequency at 15 MHz. Moreover, the motion system is composed of Aerotech devices of 0.5 μm step accuracy.

(a) (b)

Fig. 3. Clone mosaic icon that simulates the technique of the ones in Hagia Sophia, Constantinople. (a) The hidden mosaic pattern under (b) thick mortar covering.

An initial tomographic image of the clone mosaic is depicted in Fig.4. It is evident that the acoustic waves are able to penetrate the thick mortar and provide high fidelity information of the underneath tesserae. Specifically, the mortar is appearing as the high intensity upper layer due to its scattering, while the thickness seems decreased due to the high acoustic velocity. On the other hand, tesserae are appearing as separated elements of varying intensity

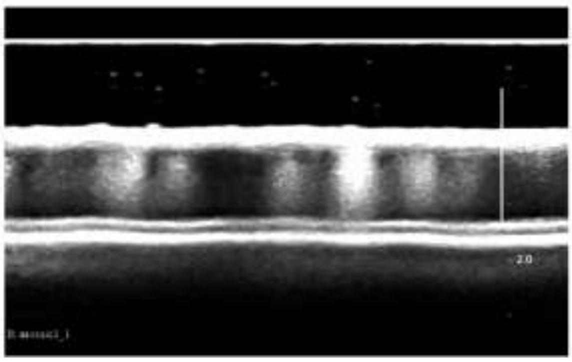

Fig. 4. A tomographic image of the clone mosaic acquired using ultrasonic phased array system at 20 MHz.

The 3D image reconstruction from the tomographic sequence of constant velocity motion of the ultrasonic probe is, then, extracted considering our proposed methodology. The outcome is demonstrated in Fig. 5 using the flexible 3D-SLICER software. Here, the image is displayed in two phases, namely the upper mortar part in Fig. 5a and the inner mosaic one in Fig.5b. The former is an impressively detailed illustration of the mortar surface, where even the roughness of this layer can be evaluated.

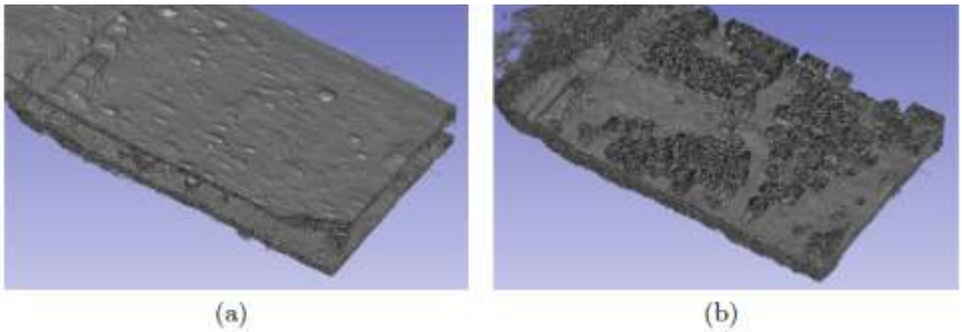

Fig. 5. (a) Detail of the clone mosaic at the region of interest and (b) an horizontal slice of the acquired measurement at the same region

However, the most interesting results are revealed through the mosaic region that is optically hidden under the mortar. It is observable that the tesserae shape is reconstructed successfully, while the detailed pattern of the mosaic is, also, evaluated. The last remark is validated in Fig. 6, where a horizontal slice of the 3D image at the tesserae region is extracted and compared to the original mosaic of Fig. 3a. Here, one can note that the reconstructed mosaic pattern is identical to the original, thus proving the potential of the proposed instrumentation and the subsequent processing methodology.

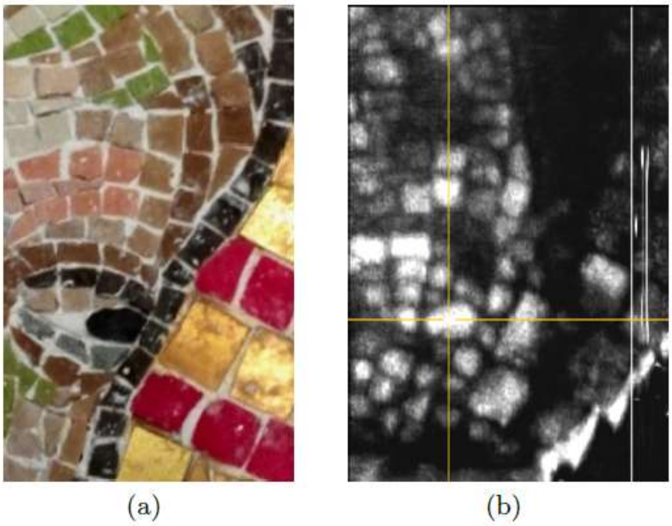

Fig. 6. (a) Detail of the clone mosaic at the region of interest and (b) an horizontal slice of the acquired measurement at the same region

3.3 Vertical resolution

The final step of our analysis is the investigation of the ultrasonic vertical resolution, since the horizontal one depends on the motion plan of Section 2.2. It is well-known that the vertical resolution is influenced mainly by the frequency, but the phased array setup and the multi-line acquisition beam forming scheme are able to improve the outcome. To this end, the inner details of a tessera is examined in Fig. 7, revealing the structure scratches due to its preparation method. This interesting result is compared to a single tessera analysis of Fig. 7a that is measured using an ultrasonic probe at 175 MHz. The reconstructed image from this measurement is depicted in Fig. 7b, where corresponding structure scratches are observed. Consequently, despite the decreased frequency of the phased array probe, significant vertical details of the inner structure can be evaluated.

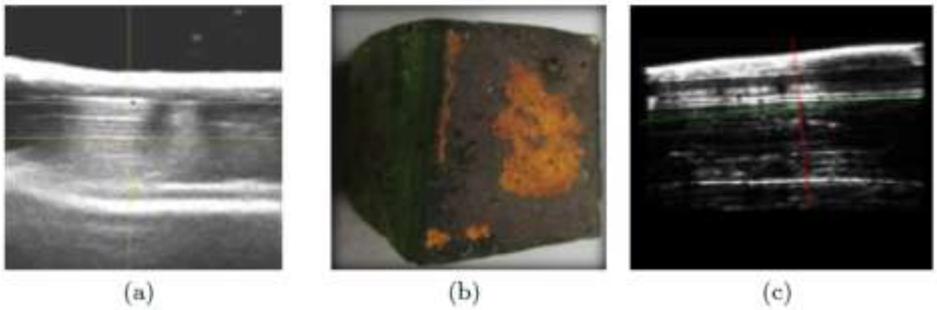

Fig. 7. (a) Details of a tessera inside the clone mosaic acquired using ultrasonic phased array system at 20MHz. (b) A single tessera from the archaeological site of Ancient Messene and (c) tomography of its inner structure using acoustic microscopy with transducer at 175 MHz.

4 Conclusion

The instrumentation and the subsequent processing methodology for the non- destructive 3D tomographic reconstruction of iconic cultural heritage assets has been proposed in this work. The basic parts of the instrumentation include an ultrasonic phased array system and appropriate mechanical adaptations for its motion planning towards the object that is under investigation. Then, powerful methods, such as the multi-line acquisition beam forming, are applied to extract the 3D inner reconstruction of the object. The utilization of the proposed methodology on a clone mosaic that is hidden under thick mortar, verified the successful implementation indicating the method's potential.

Acknowledgment

This work is part of Iperion HS project that has received funding from the European Union Horizon 2020 Framework Programme under grant agreement no. 871034.

References

1. ASTM, A.E.: 2339, standard practice for digital imaging and communication in nondestructive evaluation (diconde) (2011)

2. Karagiannis, G., Alexiadis, D.S., Damtsios, A., Sergiadis, G.D., Salpistis, C.: Three-dimensional nondestructive “sampling” of art objects using acoustic microscopy and time–frequency analysis. IEEE Transactions on Instrumentation and Measurement 60(9), 3082–3109 (2011)
3. Karagiannis, G., Karamanos, T., Athanasopoulos, E., Panayiotou, K., Amana- tiadis, S., Apostolidis, G., Karagiannis, T.: Development of an itomography infras- tructure for non-destructive documentation of cultural heritage objects. In: 2018 IEEE International Conference on Imaging Systems and Techniques (IST). pp. 1–6. IEEE (2018)
4. Pieper, S., Halle, M., Kikinis, R.: 3d slicer. In: 2004 2nd IEEE international sympo- sium on biomedical imaging: nano to macro (IEEE Cat No. 04EX821). pp. 632–635. IEEE (2004)
5. Shattuck, D.P., Weinshenker, M.D., Smith, S.W., von Ramm, O.T.: Explososcan: A parallel processing technique for high speed ultrasound imaging with linear phased arrays. The Journal of the Acoustical Society of America 75(4), 1273–1282 (1984)
6. Smith, S.W., Pavy, H.G., von Ramm, O.T.: High-speed ultrasound volumetric imaging system. i. transducer design and beam steering. IEEE transactions on ultrasonics, ferroelectrics, and frequency control 38(2), 100–108 (1991)
7. Snyder, J.E., Kisslo, J., von Ramm, O.T.: Real-time orthogonal mode scanning of the heart. i. system design. Journal of the American College of Cardiology 7(6), 1279–1285 (1986)
8. Treeby, B.E., Cox, B.T.: k-wave: Matlab toolbox for the simulation and reconstruction of photoacoustic wave fields. Journal of biomedical optics 15(2), 021314 (2010)
9. Von Ramm, O.T., Smith, S.W., Pavy, H.G.: High-speed ultrasound volumetric imaging system. ii. parallel processing and image display. IEEE transactions on ultrasonics, ferroelectrics, and frequency control 38(2), 109–115 (1991)
10. Wolf, I., Vetter, M., Wegner, I., Nolden, M., Bottger, T., Hastenteufel, M., Schobinger, M., Kunert, T., Meinzer, H.P.: The medical imaging interaction toolkit (mitk): a toolkit facilitating the creation of interactive software by extending vtk and itk. In: Medical Imaging 2004: Visualization, Image-Guided Procedures, and Display. vol. 5367, pp. 16–27. International Society for Optics and Photonics (2004)